Observation of Tunable Refractive Indices and Strong Intermolecular Interactions in Newly Synthesized Methylene-biphenylene-Bridged Silsesquioxane Thin Films

ARTICLE *in* THE JOURNAL OF PHYSICAL CHEMISTRY C · JULY 2010

Impact Factor: 4.77 · DOI: 10.1021/jp909287f

4 AUTHORS, INCLUDING:

Hyun-Dam Jeong
Chonnam National University
47 PUBLICATIONS **375** CITATIONS

SEE PROFILE

Observation of Tunable Refractive Indices and Strong Intermolecular Interactions in Newly Synthesized Methylene-biphenylene-Bridged Silsesquioxane Thin Films

Jin-Kyu Choi, Duck-Hee Lee, Soon-Ki Rhee, and Hyun-Dam Jeong*

Department of Chemistry, Chonnam National University, Gwangju, 500-757, Republic of Korea

Received: September 28, 2009; Revised Manuscript Received: July 11, 2010

A series of methylene-biphenylene-bridged silsesquioxane thin films were synthesized from 4,4′-bis(trimethoxysilylmethyl)biphenyl (MBP) and methyltrimethoxysilane (MTMS) monomers at different molar ratios. A sol−gel process employing hydrolysis and condensation reactions was used to synthesize the precursors that were then spin-coated onto a silicon wafer. Optical properties of the thin films were investigated using spectroscopic ellipsometry (SE). Refractive index values increased from 1.40 for 0 mol % MBP to 1.60 for 100 mol % MBP. These are promising results for reliable encapsulants for a high-performance white light emitting diode (LED) given its high refractive index value and absence of epoxy moieties. The dielectric functions, consisting of real and imaginary parts closely related to refractive index and extinction coefficient, were also investigated. A new peak at 3.96 eV was observed for the 75 and 100 mol % MBPs in the imaginary dielectric functions, which was absent for the 25 and 50 mol % MBPs. The main origin for the new peak was thought to be the same as that for the peak at 4.67 eV, from the pseudo $B_{1u} \leftarrow A_{1\ g}$ transition of the six-membered ring constituting the biphenyl group. Herein, we suggest that the peak at 3.96 eV is generated from interactions between the biphenyl rings in the silsesquioxane materials, which can be explained by the local field correction and/or the planarization models.

Introduction

White light emitting diodes (LEDs) are a promising next-generation lighting source given their advantages over traditional incandescent and fluorescent sources. However, such LEDs are not without problems, particularly regarding performance and lifetime, some of which originate from the encapsulant materials used in LED device construction. Epoxy resins are employed as standard encapsulant materials and work well for optical efficiency and low cost means; however, they give rise to several problems in high-drive-current applications.[1] First, the maximum operating temperature for an epoxy-encapsulated LED lamp is limited to 10−20 °C below the glass transition temperature (T_g) of the epoxy resin, typically between 100 and 150 °C. For example, the T_g of diglycidyl ether of bisphenol A (DGEBA) is reported to be 135 °C.[2] The thermal expansion coefficient (CTE) of DGEBA is 50 um/m °C below its T_g and 160 um/m °C above its T_g.[2] Therefore, when the operating temperature for the DGEBA-encapsulated LED is higher than the T_g of DGEBA, high stress is generated, causing failure of the thin Au wire or epoxy encapsulation delamination.[1,3] Thus, epoxy encapsulants are unsuitable for the high-drive-current applications where heat dissipation is a serious problem in LED devices. The second problem is their tendency to yellow when exposed to intense blue or ultraviolet (UV) light, or aged thermally. This yellowing is due to thermal decomposition of molecules in the epoxy encapsulant that obviously decreases light transparency and reduces the light extraction efficiency.[1,4−7] To overcome these problems, silicone materials that include epoxy or other organic moieties have been developed, possessing improved light and thermal aging stabilities.[6,8−11] The refractive indices of conventional silicone materials are known to range from 1.3 to 1.5,[12] which is significantly deficient for the encapsulant applications. As a result, the light extraction efficiency of LEDs encapsulated by silicone-modified epoxy materials is fundamentally limited.[13,14] This occurs because as the refractive index (n) of the encapsulant increases the light-extraction efficiency increases rapidly. Typically, in an LED device of III−V nitrides and phosphides ($n = 2.5-3.5$),[13] the light-extraction efficiency is estimated at approximately 30%, with transparent epoxy encapsulants with refractive indices of 1.4, and increases anywhere from 42 to 48% for refractive indices of 1.6 and 1.7.[15]

Organic-bridged silsesquioxanes are a class of organic−inorganic hybrid materials that integrate organic and inorganic groups at the molecular level, resulting in unique molecular structures that include a variable organic bridging group and two or more trifunctional silyl groups.[16−18] These materials garnered much interest due to the thermal[19,20] and mechanical[21] stabilities of the inorganic component and the capability of modifying bulk properties by varying the organic component.[7,17,22−26] In detail, variation of organic species at the molecular level can be used to tune bulk properties such as optical properties,[7,17,22,23] including refractive index and light absorption properties, important factors for LED encapsulant application, dielectric properties,[24,25] and chemical functions.[26] There have been many efforts to apply the organic-bridged silsesquioxane materials to optical devices,[27−31] high-capacity absorbents,[32−34] 3-D information storage media,[35] and proton-conducting media for fuel cells.[36,37]

In this article, to develop new, high-performance encapsulants lacking epoxy moieties capable of causing Au wire failure and the aforementioned yellowing, organic-bridged silsesquioxane thin films with high-refractive indices have been synthesized. The thin films were synthesized from methyltrimethoxysilane (MTMS) and 4,4′-bis(trimethoxysilylmethyl)biphenyl (BTMSMBP; abbreviated as MBP in the following section) monomers through hydrolysis and condensation polymerization (Scheme 1). In the resulting organic-bridged silsesquioxane thin

* Corresponding author. E-mail: hdjeong@chonnam.ac.kr. Tel.: 2-530-3387. Fax: 82-62-530-3389.

10.1021/jp909287f
Published on Web 07/29/2010

SCHEME 1: Schematic Diagram of the Synthesis of the Methylene-biphenylene-Bridged Silsesquioxane Thin Films Using Hydrolysis and Condensation Polymerization with the MBP and the MTMS Monomers, Followed by a Spin-Coating Process

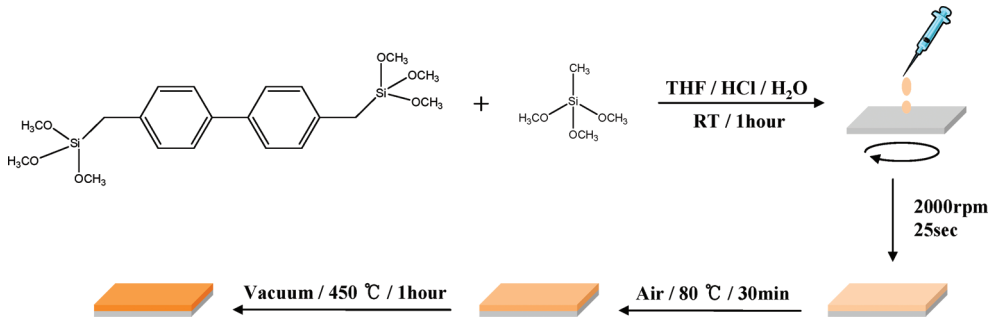

films, the biphenyl groups were responsible for increasing the refractive index, owing to their π electron clouds, while the remaining $-SiO_{3/2}-$ structures were necessary for thermal and mechanical stability. In addition, the $-SiO_{3/2}-$ structures were predicted to be optically inert given their inherently high band gap, with values varying from 4.59 to 7.27 eV according to the involved alkyl groups,[38,39] when compared to the photon energies of the visible ranges (1.59−3.27 eV).

In this article, this lab has characterized the methylene-biphenylene-bridged silsesquioxane thin films synthesized by hydrolysis and condensation polymerization. Herein, the necessary thermal and mechanical stabilities could be satisfied by introducing a −Si−O− inorganic moiety that was also predicted to be optically inert given its inherently high band gap. A high refractive index was predicted to arise from the organic moiety of π-electron-containing aromatic groups. This material design concept is very promising for application toward encapsulant materials of white LEDs given the simple synthetic and fabrication conditions. Most interestingly, a new peak was observed in the imaginary part of the complex dielectric function, indicating strong intermolecular interaction between the bridged biphenylene groups.

Experimental Section

Syntheses of Methylene-biphenylene-Bridged Silsesquioxane Precursor Solutions. All chemicals were used as received without further purification. 4,4′-Bis(trimethoxysilylmethyl)biphenyl (MBP, 98%) and methyltrimethoxysilane (MTMS, 98%) were purchased from JSI Silicone (Seongnam-si, South Korea) and Aldrich (St. Louis, MO, USA), respectively. Tetrahydrofuran (THF, 99.5%) was obtained from Duksan (Ansan-si, South Korea). The syntheses of the methylene-biphenylene-bridged silsesquioxane precursors were performed at room temperature in a closed vial and cleaned with ethanol and acetone, by varying the molar ratio of MBP and MTMS (viz., [MBP]:[MTMS] = 10:0 (0.64 g:0 g); 7.5:2.5 (0.48 g:0.05 g); 5:5 (0.32 g:0.10 g); 2.5:7.5 (0.16 g:0.16 g); 0:10 (0.00 g:0.21 g)), as summarized in Table 1. The MBP and MTMS were dissolved in 3.0 g of THF, respectively. Then, the two solutions were mixed together under stirring, followed by addition of 0.25 M HCl at 0.37, 0.32, 0.28, 0.23, and 0.18 g, respectively. After stirring for 1 h at room temperature, the final precursor solutions were obtained.

Film Preparation. After filtration (PTFE, 0.25 um), the precursor solutions were spin-coated on a p-type Si(100) wafer (resistivity, 1−30 Ω·cm; thickness, 525 nm) at 2000 rpm for 25 s with a spin-coater (SPIN 3000, MIDAS SYSTEM Co., Ltd., Daejeon-si, South Korea). The Si wafers were purchased from Silicon Valley Microelectronics, Inc. (Santa Clara, CA, USA), with resistivity and thickness values provided by the same company, and used after a brief rinsing of the surface with ethanol and acetone to remove organic residues. The films were then heated at 80 °C on a hot plate for 30 min in an open atmosphere to remove any remaining solvent. Finally, the films were cured for 1 h at 450 °C in a vacuum tube furnace (SH-TMFGF, SAMHEUNG ENERGY, Gyeonggi-do, South Korea) under a pressure of approximately 1.0×10^{-2} Torr.

TABLE 1: Composition of Precursor Solutions Used for Preparing the Methylene-biphenylene-Bridged Silsesquioxane Thin Films[a]

	MBP	MTMS	0.25 M HCl	THF
MBP 100 mol %	0.64 g	0.0 g	0.37 g	6.0 g
MBP 75 mol %	0.48 g	0.05 g	0.32 g	6.0 g
MBP 50 mol %	0.32 g	0.10 g	0.28 g	6.0 g
MBP 25 mol %	0.16 g	0.16 g	0.23 g	6.0 g
MBP 0 mol %	0.0 g	0.21 g	0.18 g	6.0 g

[a] $\frac{[HCl]}{[OMe]} = 0.01, \quad \frac{[H_2O]}{[OMe]} = 2.22$

.

Film Characterization. Fourier transform infrared spectroscopy (FT-IR) was implemented to investigate the molecular structure of the final methylene-biphenylene-bridged silsesquioxane thin films. The measurements were conducted on a Nicolet 380 spectrometer (Waltham, MA, USA) operated in the mid-IR range of 4000−400 cm^{-1}, with all spectra obtained at a spectral resolution of 7.7 cm^{-1} in transmittance mode. To investigate compositional changes by varying the molar ratio of MBP and MTMS, X-ray photoelectron spectroscopy (XPS) measurements were conducted on a MultiLab 2000 (Waltham, MA, USA) using a Mg Kα (1253.6 eV) source at a pass energy of 20 eV, under a pressure of 1.0×10^{-9} Torr. An Ar^+ ion gun sputtering of 2 min at a power of 2 kV and 1.3 μA was used for a brief cleaning of the surface of the samples prior to XPS measurements. The thicknesses and refractive indices of the methylene-biphenylene-bridged silsesquioxane thin films were measured by spectroscopic ellipsometry (SE) with a M2000D (J.A. Wollam Co. Inc., Lincoln, NE, USA).

Results and Discussion

As the molar concentration of the MBP under the current synthetic conditions increased, the more the biphenyl groups became involved in the organic−silsesquioxane hybrid films, as confirmed by the FT-IR and XPS results. Figure 1 shows the FT-IR spectra of the methylene-biphenylene-bridged silsesquioxane thin films with a variation in molar concentration

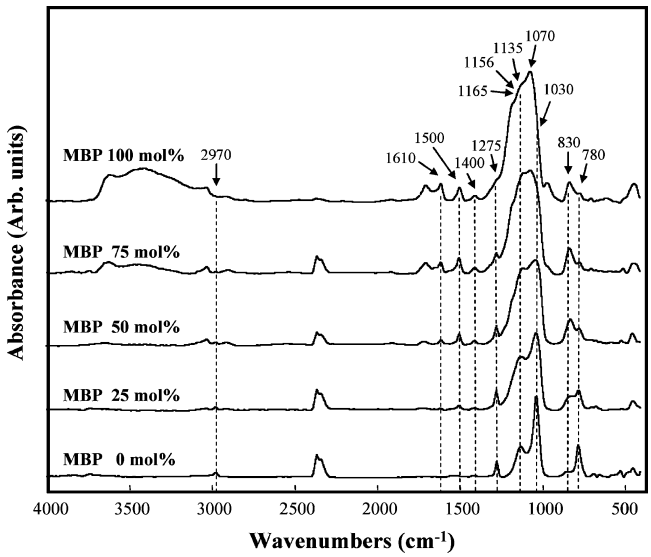

Figure 1. FT-IR spectra of the methylene-biphenylene-bridged silsesquioxane thin films with variation in the MBP molar concentration.

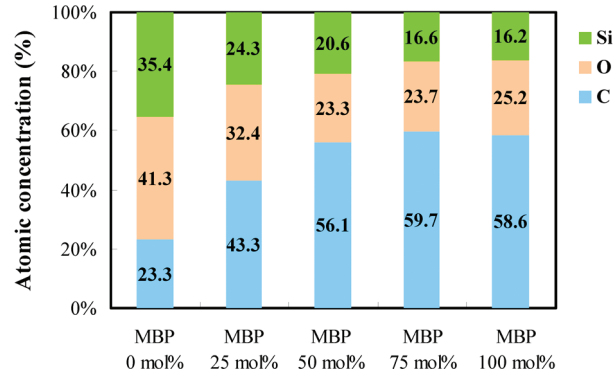

Figure 2. XPS quantification results showing variation in the atomic concentration of the methylene-biphenylene-bridged silsesquioxane thin films with variation in the molar concentration of the quantified MBP. As the molar concentration of the MBP in the synthetic conditions increased, the atomic concentration percentage of the carbon element increased, indicating greater involvement of the biphenyl rings in the films.

of the MBP. Increase in the intensities of the C═C stretching peaks at 1610 and 1500 cm^{-1}, the C−Ph stretching peak at 1165 cm^{-1}, the biphenyl C−H vibration peaks at 1156 and 1400 cm^{-1}, with peaks at 1165 and 1156 cm^{-1} overlapping with other peaks, and the out-of-plane C−H wag peak of the biphenyl at 830 cm^{-1} indicated an elevated concentration of the biphenyl ring in the thin film upon increase in MBP molar concentration.[40−43] In addition, the intensities of the MTMS peak indicators, the C−H_3 stretching peak at 2970 cm^{-1}, the Si−CH_3 bending peak at 1275 cm^{-1}, and the Si−C stretching peak at 780 cm^{-1}, decreased when the molar concentration of the MTMS decreased.[44]

Silsesquioxane materials have been considered organic−inorganic hybrids that combine many of the desirable properties of conventional organic and inorganic components, such as sound photostability, thermal stability, and chemical resistance. As such, they have been applied toward low dielectric constant interlayer dielectric materials and photonic materials for waveguides and devices.[24−26,45−51] These materials were also reported to possess various structures, including random, ladder, cage, and partial cage.[45,52] The methylene-biphenylene-bridged silsesquioxane resin presented herein inherently possesses these structure types that could be investigated by characteristic peaks in the range of 1200−1000 cm^{-1} of the FT-IR spectra, related to Si−O−Si stretching. In the case of 0 mol % MBP, there were two absorption peaks at 1135 and 1030 cm^{-1} attributed to the Si−O−Si stretching in cage-like and network-like structures, respectively.[45,53,54] The 1030 cm^{-1} peak of a network-like structure was interpreted to arise from a breakdown in symmetry of a highly symmetric cage structure, originally showing only one peak at ∼1135 cm^{-1}.[45] The peak at 1030 cm^{-1} for 0 mol % MBP shifted to 1070 cm^{-1} for 100% MBP. According to the central force model, this peak shift was related to the changes in bonding characteristics, such as bond angle and length, where the frequency of the Si−O−Si stretching peak in amorphous SiO_2 could be approximated by the following equation[55]

$$v^2 = (k/m_0)[\sin^2(\theta/2)]$$

where k is a nearest-neighbor effective force constant variable with the Si−O bond length, m_0 the mass of an oxygen atom, and θ the Si−O−Si bond angle. Assuming that variation of the Si−O bond length is small, this equation can be simplified accordingly[55]

$$\nu = \nu_0 \sin(\theta/2)$$

where ν_0 = 1135.6 cm^{-1} is experimentally obtained for ν = 1080 cm^{-1} in thermally grown SiO_2 films. Therefore, with the above approximation, the peaks at 1030 cm^{-1} for 0 mol % MBP and 1070 cm^{-1} for 100 mol % MBP are interpreted to correspond to the bond angles of 130° and 141° for Si−O−Si stretching in the network-like structures, respectively. This higher Si−O−Si angle value for the higher MBP molar concentration was thought to be due to the angle strain induced from the strong intermolecular repulsion between the biphenyl groups. In addition, the ratio of the peak intensity for the cage-like structure near 1135 cm^{-1} to that for the network-like structure between 1070 and 1030 cm^{-1} increased with increasing MBP molar concentration, as shown in Figure 1, indicating that methylene-biphenylene groups in the silsesquioxane thin films tended to induce more cage-like structures.

To investigate the microstructures of the methylene-biphenylene-bridged silsesquioxane materials, solid state ^{29}Si NMR measurements were performed (Supporting Information, Figure S1 and Table S1). The 0 mol % MBP thin film showed two peaks at −59.1 and −68.1 ppm, assignable to the respective T^2 [$RSi(OR)_1(O_{1/2})_2$] and T^3 [$RSi(O_{1/2})_3$] species.[53,56] The 100 mol % MBP thin film showed three peaks at −51.7, −62.4, and −73.8 ppm that could be assigned to the T^1 [$RSi(OR)_2(O_{1/2})_1$], T^2, and T^3 species, respectively (Supporting Information, Figure S1).[17,57] Then, the degree of condensation (DC) values for the 0 and 100 mol % MBP thin films were simply calculated with the areas of each T^n peak (n = 0−3),[58] at which the overlapped peaks were deconvoluted assuming Gaussian/Lorentzian peaks to give a DC of 97.4 and 87.5% for the 0 and 100 mol % MBP thin films, respectively (Supporting Information, Table S1). This indicated that the 0 mol % MBP thin film was more condensed than the 100 mol % thin film.

The variation in the atomic concentration of the methylene-biphenylene-bridged silsesquioxane thin films with a molar concentration of the MBP is shown in the XPS quantification results of Figure 2. As the molar concentration increased, the

atomic concentration percentage of carbon increased, indicating greater involvement of the biphenyl rings in the films.

Spectroscopic ellipsometry (SE) was performed to measure refractive index (n), extinction coefficient (k), and thickness of the methylene-biphenylene-bridged silsesquioxane thin films. Spectroscopic ellipsometry was selected as it is a nondestructive and powerful technique capable of investigating the optical response of materials and, particularly, of simultaneously measuring the thickness and optical constants of a multilayer system when suitable modeling approaches have been developed. Ellipsometric data (I_S/I_C), as defined below, were obtained at three incidence angles of 65°, 70°, and 75° and in a spectral range of 200−1000 nm. The I_S and I_C are related to the ellipsometric angles Ψ and Δ, defined in the fundamental equation of ellipsometry as[59]

$$\rho = \frac{r_p}{r_s} = \tan\psi \cdot \exp(i\Delta)$$
$$I_s = \sin(2\psi)\cdot\sin(\Delta)$$
$$I_c = \sin(2\psi)\cdot\cos(\Delta)$$

where s oscillates perpendicular to the plane of incidence and p oscillates parallel to the plane of incidence. The r_p and r_s values are the complex Frensel reflection coefficients, parallel and perpendicular to the plane of incidence. In the data collection process, the experimental SE data (I_S/I_C) were measured, while the fitting process was used to adjust the theoretical fitting coefficients to the experimental data until the best fit was determined through the χ^2 (goodness of fit) minimization process. Both the film optical constant and thickness were simultaneously obtained from the SE data analysis. In this experiment, the Tauc−Lorentz model[60] was utilized as a model for the fitting process.

Figure 3 shows variations in refractive index, extinction coefficient, and thickness of the methylene-biphenylene-bridged silsesquioxane thin films obtained from the SE measurements. As shown in Figure 3a and 3c, when the [MBP]:[MTMS] ratios were 10:0, 7.5:2.5, 5:5, 2.5:7.5, and 0:10, the corresponding thicknesses of the resultant thin films were estimated to be 568, 462, 372, 264, and 118 nm, respectively, while the refractive indices turned out to be 1.64, 1.62, 1.58, 1.54, and 1.41 at a wavelength of 460 nm, and 1.60, 1.59, 1.55, 1.52, and 1.40 at a wavelength of 633 nm. The refractive indices of the hybrid films at a wavelength of 633 nm increased systematically from 1.40 for a MBP molar concentration of 0% to 1.60 for 100%. This increase was attributed to the anticipated electronic polarization of the biphenyl groups. The light-extraction efficiency was estimated at approximately 30% with the use of transparent epoxy encapsulants with a refractive index of 1.4 and at 42% for a refractive index of 1.6.[15] Therefore, the hybrid film from the 100% MBP molar concentration was sufficiently applicable in terms of refractive indices but only if the light and thermal aging stabilities and mechanical stabilities were confirmed in the actual white LED devices.

The electronic polarization of the π electron clouds in the biphenyl groups that resulted in the high refractive indices was closely related to the electronic transitions between the electronic energy levels (π orbitals of the molecules).[61,62] In the optical theory of solids of view, the refractive index n and extinction coefficient k, which vary with wavelength (λ), form the complex refractive index: $N(\lambda) = n(\lambda) + ik(\lambda)$.[63,64] The light-scattering and light-absorbing capacities of the materials depend on n and k, respectively. Alternatively, the interaction with materials can

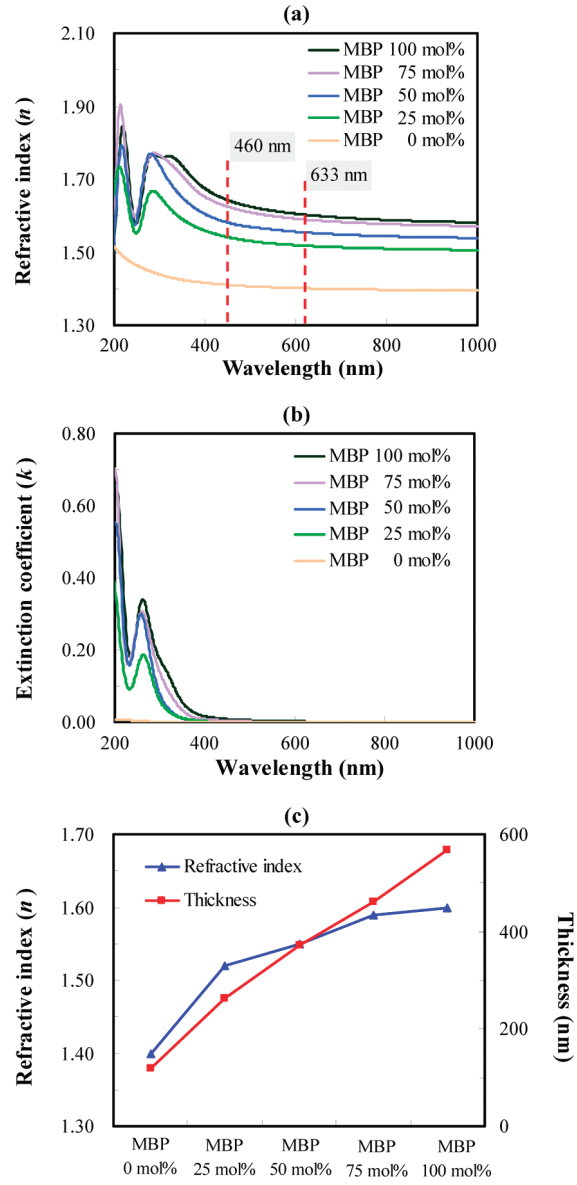

Figure 3. SE results: (a) variation in refractive index (n) of the methylene-biphenylene-bridged silsesquioxane thin films with variation in the molar concentration of the MBP; (b) variation in extinction coefficient (k) of the methylene-biphenylene-bridged silsesquioxane thin films with variation in the molar concentration of the MBP; (c) refractive indices at a wavelength of 633 nm systematically increased from 1.40 for a MBP molar concentration of 0% to 1.60 at 100%.

be treated in terms of a complex dielectric function, $\varepsilon(\lambda) = \varepsilon_1(\lambda) + \varepsilon_2(\lambda)$, which represents the linear response of the electronic structure of an insulating material toward the electric field of the incident radiation. The real part, $\varepsilon_1(\lambda)$, is associated with the electronic polarizability of the material, while the imaginary part, $\varepsilon_2(\lambda)$, is related to electronic absorption of the material. The values of n and k are related to ε_1 and ε_2 as follows[63,64]

$$\varepsilon_1 = n^2 - k^2, \varepsilon_2 = 2nk \quad (1)$$

$$n = \frac{(\varepsilon_1 + (\varepsilon_1^2 + \varepsilon_2^2)^{0.5})^{0.5}}{\sqrt{2}}, k = \frac{(-\varepsilon_1 + (\varepsilon_1^2 + \varepsilon_2^2)^{0.5})^{0.5}}{\sqrt{2}} \quad (2)$$

In semiconductors and insulators, optical transitions induced by electromagnetic fields can be explained by assuming the

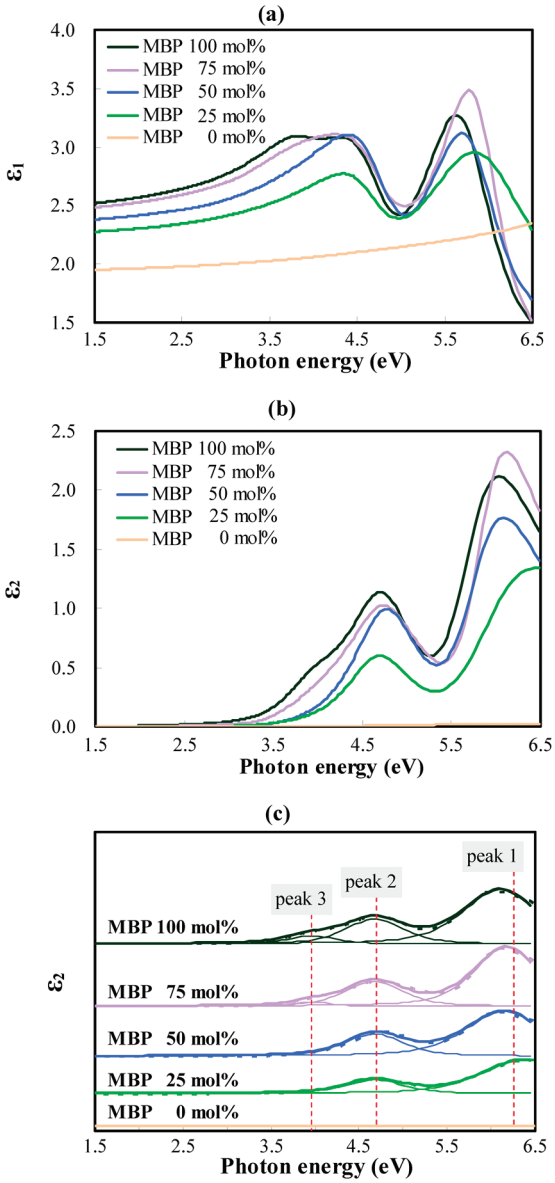

Figure 4. (a) Variation in the real part (ε_1) of the dielectric functions calculated from the refractive index (n) and extinction coefficient (k). (b) Variation in the imaginary part (ε_2) of the dielectric functions calculated from the refractive index (n) and extinction coefficient (k) ($\varepsilon_2 = 2nk$). (c) Gaussian/Lorentzian deconvolutions of the imaginary part (ε_2) of the dielectric functions. Dotted and solid lines are original and deconvolution graphs, respectively. Compared to 0, 25, and 50 mol % MBP samples, the 75 and 100 mol % MBP samples showed a new peak (peak 3) centered at 3.96 eV (314 nm), thought to be due to intermolecular interactions between the biphenyl groups.

response of a classical harmonic oscillator based on a classical dispersion theory derived mostly from Drude, Voigt, and Lorentz, generally referred to as the Lorentz oscillator model.[59,65,66] Herein, the dielectric function is simply expressed by physical parameters of the oscillators as follows: $-f_i$, ω_{oi}, and γ_i are oscillator strength, resonant frequency, and the damping coefficient of oscillator i, while m_i and e are electron mass and charge

$$\varepsilon_1 = 1 + \sum_i S_i \frac{(\omega_{oi}^2 - \omega^2)}{(\omega_{oi}^2 - \omega^2)^2 + \gamma_i^2\omega^2},\ S_i = \frac{4\pi N_i e^2 f_i}{m_i} \quad (3)$$

$$\varepsilon_2 = \sum_i S_i \frac{\gamma_i \omega}{(\omega_{oi}^2 - \omega^2)^2 + \gamma_i^2\omega^2} \quad (4)$$

This model is generally applicable in real systems as the corresponding quantum-mechanical equation for ε and has the same form as the classical equation of the damped oscillator.[67]

The ε_1 and ε_2 data for the presented organic−silsesquioxane hybrid thin films were calculated from the n and k data using eq 1, as shown in Figure 4. In the 25 and 50 mol % MBP samples, there were two oscillators in the range of 2.5−6.5 eV, corresponding to approximately 6.2 (200 nm) and 4.67 eV (266 nm) and, respectively, denoted as peak 1 and peak 2 (Figure 4c). The former oscillator was closely related to the $B_{2u} \leftarrow A_{1g}$ transition, while the latter originated from the $B_{1u} \leftarrow A_{1g}$ transition.[68] In the 75 and 100 mol % MBP samples, a new peak (peak 3) centered at 3.96 eV (314 nm) was observed, thought to be due to intermolecular interactions between the biphenyl groups. The intensities of these three peaks were plotted with the MBP molar concentration (Figure 5), where the total intensities of peak 2 and peak 3 correlated well to the MBP molar concentration, indicating that both peaks were attributed to the biphenyl rings. Verily, in the 75 and 100 mol % MBP samples, there were two kinds of biphenyl groups, depending upon whether or not a biphenyl ring experienced intermolecular interactions with another ring.

To determine how the molecular interaction between the biphenyl groups generated peak 3, which was of lower energy compared to peak 2, it was tentatively assumed that, in the presented silsesquioxane thin films, as the molar concentration of the MBP increased, there were many more chances for the two adjacent biphenyl groups to experience intermolecular interactions. To explain the appearance of peak 3 owing to such intermolecular interactions, two possible models were thus suggested: one from a local field correction and the other related to planarization of neighboring phenyl rings.

1. Local Field Correction Model.[65,69] Oscillating electrons in the oscillator from a biphenyl group, giving rise to peak 2, experience new electric fields from other electrons of other, close, neighboring biphenyl rings. An electrostatic calculation taking into account this mutual interaction leads to the following expression for the imaginary dielectric function (ε_2) for the corresponding oscillator of the silsesquioxane thin films

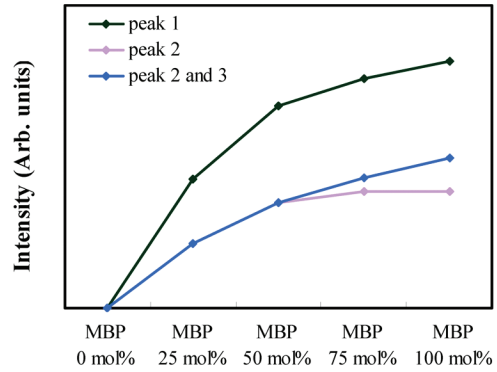

Figure 5. (a) Plots of the molar concentration of MBP with intensities of peak 1. (b) Plots of the molar concentration of MBP with intensities of peak 2. (c) Plots of the molar concentration of MBP with intensities of peak 2 and peak 3. Total intensity of peak 2 and peak 3 is well correlated with the molar concentration of MBP due to the origin of both peaks from the biphenyl rings.

$$\varepsilon_2 = S\frac{\gamma\omega}{(\omega_o'^2 - \omega^2)^2 + \gamma^2\omega^2},\ \omega_o'^2 = \omega_o^2 - \frac{1}{3}S \quad (5)$$

$$\varepsilon_2 = S\frac{\gamma\omega}{\left(\omega_o^2 - \frac{1}{3}S - \omega^2\right)^2 + \gamma^2\omega^2} \quad (6)$$

This ω_o' has been shifted down in energy from ω_o in the isolated biphenyl system, resulting from the interaction between the oscillators in those solids, through the electric field that each system produces, giving rise to peak 3.

2. Planarization of Neighboring Phenyl Rings. It is well-known that the two phenyl rings are tilted with a torsion angle between each other due to the steric repulsion of the *ortho* position hydrogen atoms.[70−73] In the ground state of the equilibrium geometry of the biphenyl molecule, the torsion angle between the two phenyl rings has been reported to be 42°.[72] In a first-principle local density band structure calculation on crystalline poly(*para*-phenylene), the torsion angle between the adjacent phenyl rings was estimated to be 27°.[73] Interestingly, the band gap of the material varied upon changing the torsion angle of the two phenyl rings, 3.75 and 3.38 eV, respectively, for torsion angles of 27° and 0°. This tilted geometry was confirmed by this lab's ab initio calculations using HF/6-31(d) calculations, employing the Gaussian03 Package for the 4,4′-bis(trimethoxysilylmethyl)-biphenyl molecule (Figure 6).[74] The torsion angle of the phenyl rings in the optimized geometry was determined to be 43.8°. It is very reasonable that the intermolecular interaction of the two adjacent biphenyl groups, approaching each other very closely (an alleged face-to-face $\pi-\pi$ interaction), enforced planarization of the biphenyl groups. Because the emphasis in this work is the "direct" intermolecular interaction of two biphenyl rings, this explanation differs somewhat from previous studies where, in biphenyl systems, a more planar conformation was favored in the crystalline environment or aggregation state associated with indirect intermolecular interaction between the biphenyl rings.[75,76] Then, at high MBP molar concentrations, there were relatively higher amounts of coplanar biphenyl groups relative to low MBP molar concentrations. Since the coplanar biphenyl groups were apt to have HOMO−LUMO gaps lower than those tilted, because of their torsion angle being near 0°,[73] peak 3 in the imaginary dielectric function graphs was observed at high MBP molar concentrations (Figure 4c), as mentioned above.

In addition to the two proposed models, there exists another explanation for the 3.96 eV peak in the ε_2 data. An expert in the silsesquioxane materials area might consider a conjugation through the $-SiO_{3/2}-$ structures to be the reason for the 3.96 eV feature. In the recent investigation concerning the photophysical properties of an organo-functionalized silica core, the HOMO−LUMO gap in the silica core moiety ($[SiO_{3/2}]_8$) was highly dependent on the organic group attached to the corner silicon atom.[77] For example, the values in $[HSiO_{3/2}]_8$, [phenyl−$SiO_{3/2}]_8$, and [stillbene−$SiO_{3/2}]_8$ are 6.978, 5.564, and 4.79 eV, respectively. The low gap value in [stillbene−$SiO_{3/2}]_8$ is mainly due to the interaction of LUMO or HOMO of the silica core with π^* or π orbitals of the stilbene group. However, the presented system is very different. In the biphenyl group attached through the methylene bridge to the silicon atom of a possible cage structure ($[-SiO_{3/2}]_8$), π^* or π orbitals of the biphenyl group cannot interact with the HOMO or LUMO of the $-SiO_{3/2}-$ structure because of the methylene bridge acting as a electronic spacer, preventing orbital interactions. Thus, it is the contention of the authors that the HOMO−LUMO gap in the $-SiO_{3/2}-$ structures in our materials could not been less than approximately 5 eV. This is also why the authors hold that the $-SiO_{3/2}-$ structures are optically inert and that the 3.96 eV peak is not related to the conjugation through the $-SiO_{3/2}-$ structures.

To clarify which model between the local field correction and planarization was more feasible for the current methylene-biphenylene silsesquioxane system, it was evident that further spectroscopic experiments and quantum-chemical simulations were required. Although concrete ideas have yet to be established, the authors suggest two research activities to scientists in this field. The first is to apply ultraviolet photoelectron spectroscopy (UPS) to these methylene-biphenylene-bridged silsesquioxane films, which should confirm the energy shift of the molecular orbital related to the 3.96 eV peak. The second is performing quantum-chemical calculations of the MBP dimers, where the torsion angles of the biphenyl rings and the resultant band gap values are calculated according to the varying distance between the two biphenyl rings.

Summary

In this study, a series of methylene-biphenylene-bridged silsesquioxane thin films were synthesized from 4,4′-bis-(trimethoxysilylmethyl)biphenyl (MBP) and methyltrimethoxysilane (MTMS) monomers under different molar ratios. A sol−gel process utilizing hydrolysis and condensation reactions was employed to synthesize the precursors for the thin films, followed by spin-coating onto a silicon wafer. Refractive index values of the thin films decreased from 1.60 for 100 mol % MBP to 1.40 for 0 mol % MBP; this is very promising for a reliable encapsulant for a high performance white light emitting diode (LED) given its high refractive index value and absence of epoxy moieties. The new peak at 3.96 eV in the imaginary dielectric that functioned for 100 and 75 mol % MBP, compared to 50 and 25 mol % MBP, was due to the strong intermolecular interactions between

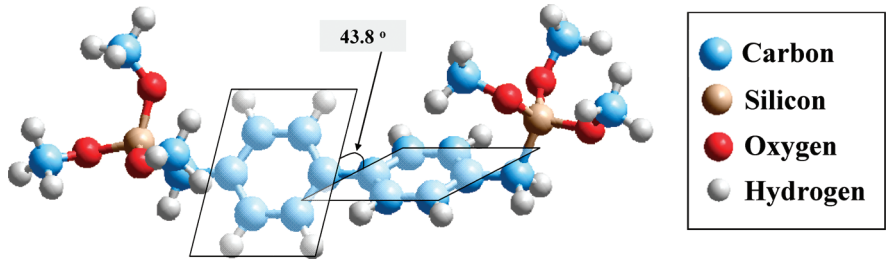

Figure 6. Tilted biphenyl rings for the 43.8° torsion angle in the 4,4′-bis(trimethoxysilylmethyl)biphenyl due to steric repulsion of the hydrogen atoms in the *ortho* position, determined from ab initio calculations using HF/6-31(d) in the Gaussian03 Package.

the adjacent biphenyl rings, modeled by local field correction and/or planarization of the biphenyl ring.

Acknowledgment. This study was financially supported by Chonnam National University, 2008.

Supporting Information Available: Solid state ^{29}Si NMR results of the methylene-biphenylene-bridged silsesquioxane materials and complete author lists of ref 1 and ref 74. This material is available free of charge via the Internet at http://pubs.acs.org.

References and Notes

(1) Steranka, F. M.; et al. *Phys. Status Solidi A* **2002**, *194*, 380.
(2) Huang, J. C.; Chu, Y. P.; Wei, M.; Deanin, R. D. *Adv. Polym. Technol.* **2004**, *23*, 298.
(3) Chin, L. W.; Hung, H. L.; Shyang, C. W. *J. Phys. Sci.* **2010**, *20*, 93.
(4) Narendran, N.; Gu, Y.; Freyssinier, J. P.; Yu, H.; Deng, L. *J. Cryst. Growth* **2004**, *268*, 449.
(5) Narendran, N.; Gu, Y. *J. Dispersion Technol.* **2005**, *1*, 167.
(6) Huang, W.; Yuan, Y.; Yunzhao, Y. *J. Adhes. Interf.* **2006**, *7*, 39.
(7) Kim, J. S.; Yang, S. C.; Bae, B. S. *Chem. Mater.* **2010**, *22*, 3549.
(8) Rubinsztajin, M. I.; Rubinsztajn Epoxy Resin Compositions, Solid State Devices Encapsulated Therewith and Method. U.S. Patent 0222298 A1, 2005.
(9) Boardman, L. D.; Thompson, D. S.; Leatherdale, C. A. Method of Making Light Emitting Device with Silicon-Containing Encapsulant. U.S. Patent 0199291 A1, 2006.
(10) Benrashid, R.; Velasco, P. High Performance Sol-Gel Spin-On Glass Materials. U.S. Patent 7393469 B2, 2008.
(11) Kim, J. S.; Yang, S. C. *J. Sol-Gel Sci. Technol* **2010**, *53*, 434.
(12) Palik, E. D. *Handbook of Optical Constants of Solids*; Academic Press: Orlando, 1985.
(13) Mont, F. W.; Kim, J. K.; Schubert, M. F.; Schbert, E. F.; Siegel, R. W. *J. Appl. Phys.* **2008**, *103*, 083120.
(14) Schubert, E. F. *Light Emitting Diodes*; Cambridge University Press: New York, 2003.
(15) Kim, K. M. www.epnc.co.kr/pdf/2007/200710/01200710034.pdf, Fig. 4.
(16) Shea, K. J.; Loy, D. A. *Chem. Mater.* **2001**, *13*, 3306.
(17) Shea, K. J.; Loy, D. A.; Webster, O. *J. Am. Chem. Soc.* **1992**, *114*, 6700.
(18) Shea, K. J.; Loy, D. A. *Polym. Mater. Sci. Eng.* **1990**, *63*, 281.
(19) Oviatt, H. W., Jr.; She, K. J.; Small, J. H. *Chem. Mater.* **1993**, *5*, 943.
(20) Hobson, S. T.; Shea, K. J. *Chem. Mater.* **1997**, *9*, 616.
(21) Lu, Y.; Fan, H.; Doke, N.; Loy, D. A.; Assink, R. A.; Lavan, D. A.; Brinker, C. J. *J. Am. Chem. Soc.* **2000**, *122*, 5258.
(22) Suratwala, T.; Gardlund, Z.; Davidson, K.; Uhlmann, D. R. *Chem. Mater.* **1998**, *10*, 190.
(23) Corriu, R. J. P.; Moreau, J. J. E.; Thepot, P.; Wong Chi Man, M.; Chorro, C.; Lere-Porte, J. P.; Sauvajol, J. L. *Chem. Mater.* **1994**, *6*, 640.
(24) Yim, J. H.; Lyu, Y. Y.; Jeong, H. D.; Mah, S. K.; Hyeon-Lee, J.; Hahn, J. H.; Kim, G. S.; Chang, S.; Park, J. G. *J. Appl. Polym. Sci.* **2003**, *90*, 626.
(25) Kim, C. S.; Jeong, H. D. *J. Phys. Chem. B* **2008**, *112*, 16257.
(26) Lee, D. H.; Jeong, H. D. *J. Phys. Chem. C* **2008**, *112*, 16984.
(27) Shea, K. J.; Moreau, J.; Loy, D. A.; Corriu, R. J. P.; Bour, B. Bridged Polysilsesquioxanes. Molecular-engineering Nanostructured Hybrid Organic-Inorganic Materials. *Functional Hybrid Materials*; Wiley Interscience: New York, 2004; pp 50−85.
(28) Choi, K. M.; Shea, K. J. *Photonic Polymer Synthesis*; Marcel Dekker: New York, 1998; pp 437−480.
(29) Innocenzi, P.; Lebeau, B. *J. Mater. Chem.* **2005**, *15*, 3821.
(30) Kagan, C. R.; Mitzi, D. B.; Dimitrakopoulos, C. D. *Science* **1999**, *286*, 945.
(31) Oviatt, H. W.; Shea, K. J.; Kalluri, S.; Shi, Y. Q.; Steier, W. H.; Dalton, L. R. *Chem. Mater.* **1995**, *7*, 493.
(32) Shea, K. J.; Hobson, S. T. J. *Hybrid Organic/Inorganic Absorbents*, 2003.
(33) Liu, J.; Feng, X. D.; Fryxell, G. E.; Wang, L. Q.; Kim, A. Y.; Gong, M. L. *Adv. Mater.* **1998**, *10*, 161.
(34) Mercier, L.; Pinnavaia, T. J. *Adv. Mater.* **1997**, *9*, 500.
(35) Huang, G. T. *Technol. Rev.* **2005**, *108*, 64.
(36) Khiterer, M.; Loy, D. A.; Cornelius, C. J.; Fujimoto, C. H.; Small, J. H.; McIntire, T. M.; Shea, K. J. *Chem. Mater.* **2006**, *18*, 3665.
(37) Honma, I.; Takeda, Y.; Bae, J. M. *Solid State Ionics* **1999**, *120*, 255.
(38) Franco, R.; Kandalam, A. K.; Pandey, R.; Pernisz, U. C. *J. Phys. Chem. B* **2002**, *106*, 1709.
(39) Rin, T.; He, C.; Xiao, Y. *J. Phys. Chem. B* **2003**, *107*, 13788.
(40) Ranganathan, T.; Gowd, E. B.; Ramesh, C.; Kumar, A. *J. Polym. Sci., Part A: Polym. Chem.* **2005**, *43*, 1903.
(41) Mathews, A. S.; Kim, D.; Kim, Y.; Kim, I.; Ha, C. S. *J. Polym. Sci., Part A: Polym. Chem.* **2008**, *46*, 8117.
(42) Bayari, S. H.; Sagdinc, S. *Struct. Chem.* **2008**, *19*, 381.
(43) Wahab, M. A.; He, C. *Langmuir* **2009**, *25*, 832.
(44) Grill, A.; Neumayer, D. A. *J. Appl. Phys.* **2003**, *94*, 6697.
(45) Baney, R. H.; Itoh, M.; Sakakibara, A.; Suzuki, T. *Chem. Rev.* **1995**, *95*, 1409.
(46) Provatas, A.; Matisons, J. G. *Trends Polym. Sci.* **1997**, *5*, 327.
(47) Hedrick, J. L.; Miller, R. D.; Hawker, C. J.; Carter, K. R.; Volksen, W.; Yoon, D. Y.; Trollsas, M. *Adv. Mater.* **1998**, *10*, 1049.
(48) Nguyen, C. V.; Carter, K. R.; Hawker, C. J.; Hedrick, J. L.; Jaffe, R. L.; Miller, R. D.; Remenar, J. F.; Rhee, H. W.; Rice, P. M.; Toney, M. F.; Trollsas, M.; Yoon, D. Y. *Chem. Mater.* **1999**, *11*, 3080.
(49) Mikoshiba, S.; Hayase, S. *J. Mater. Chem.* **1999**, *9*, 591.
(50) Buestrich, R.; Kahlenberg, F.; Popall, M.; Dannberg, P.; Muller-Fiedler, R.; Rosch, O. *J. Sol-Gel Sci. Technol.* **2001**, *20*, 181.
(51) Tadanaga, K.; Ellis, B.; Seddon, A. B. *J. Sol-Gel Sci. Technol.* **2000**, *19*, 687.
(52) Loy, D. A.; Shea, K. J. *Chem. Rev.* **1995**, *92*, 1431.
(53) Lee, L. H.; Chen, W. C.; Liu, W. C. *J. Polym. Sci., Part A: Plym. Chem.* **2002**, *40*, 1560.
(54) Cha, B. J.; Yang, J. M. *J. Appl. Polym. Sci.* **2007**, *104*, 2906.
(55) Kim, Y. H.; Hwang, M. S.; Kim, H. J.; Kim, J. Y.; Lee, Y. *J. Appl. Phys.* **2001**, *90*, 3367.
(56) Takamura, N.; Takahiro, G.; Hatano, H.; Abe, Y. *J. Polym. Sci., Part A: Polym. Chem.* **1999**, *37*, 1017.
(57) Kapoor, M. P.; Yang, Q.; Inagaki, S. *J. Am. Chem. Soc.* **2002**, *124*, 15176.
(58) Carr, S. W.; Motevalli, M.; Ou, D. L.; Sullivan, A. C. *J. Mater. Chem.* **1997**, *7*, 865.
(59) Tompkins, H. G.; McGahan, W. A. *Spectroscopic Ellipsometry and Reflectometry*; John Wiley & Sons, Inc.: New York, 1999.
(60) Fujiwara, H. *Spectroscopic Ellipsometry: Principles and applications*; John Wiley & Sons, Ltd.: Tokyo, 2003; p 171.
(61) Atkins, P.; Friedman, R. *Molecular Quantum Mechanics*, 4th ed.; Oxford University Press: New York, 2005; p 424.
(62) Kittel, C. *Introduction to Solid State Physics*, 8th ed.; John Wiley&Sons, Inc.: New York, 2005; p 466.
(63) Hummel, R. E. *Electronic Properties of Materials*, 2nd ed.; Springer: New York, 1992; p 180.
(64) Rocquefelte, X.; Goubin, F.; Koo, H. J.; Whangbo, M. H.; Jobic, S. *Inorg. Chem.* **2004**, *43*, 2246.
(65) Efimov, A. M. *Optical Constants of Inorganic Glasses*; CRC Press: Boca Raton, FL, 1995; p 6.
(66) Dressel, M.; Gruner, G. *Electrodynamics of Solids*; Cambridge University Press: New York, 2002; p 139.
(67) Chambouleyron, I.; Martinez, J. M. Optical Properties of Dielectric and Semiconductor Thin Films. *Handbook of Thin Film Materials*; Nalwa, H. S., Ed.; Academic Press: New York, 2001; Vol 3, Chap. 12.
(68) Pavia, D. L.; Lampman, G. M.; Kriz, G. S.; Vyvyan, J. R. *Introduction to Spectroscopy*, 2nd ed.; Brooks/Cole: Independence, KY, 2009; p 403.
(69) Cox, P. A. *The Electronic Structure and Chemistry of Solids*; Oxford University Press: New York, 1987; p 39.
(70) Goto, Y.; Mizoshita, N.; Ohtani, O.; Okada, T.; Shimada, T.; Tani, T.; Inagaki, S. *Chem. Mater.* **2008**, *20*, 4495.
(71) Kishimoto, N.; Hagihara, Y.; Ohni, K.; Knippenberg, S.; Francois, J. P.; Deleuze, M. S. *J. Phys. Chem. A* **2005**, *109*, 10535.
(72) Im, H. S.; Bernstein, E. R. *J. Chem. Phys.* **1988**, *88*, 7337.
(73) Ambrosch-Draxl, C.; Majewski, J. A.; Vogl, P.; Leising, G. *Phys. Rev. B.* **1995**, *51*, 9668.
(74) Frisch, M. *Gaussian03*; Gaussian Inc.: Wallingford, CT, 2005.
(75) Nam, H.; Boury, B.; Park, S. Y. *Chem. Mater.* **2006**, *18*, 5716.
(76) An, B. K.; Kwon, S. K.; Jung, S. D.; Park, S. Y. *J. Am. Chem. Soc.* **2002**, *124*, 14410.
(77) Laine, R. M.; Sulaiman, S.; Brick, C.; Roll, M.; Tamaki, R.; Asuncion, M. Z.; Neurock, M.; Filhol, J. S.; Lee, C. Y.; Zhang, J.; Goodson, T., III; Ronchi, M.; Pizzotti, M.; Rand, S. C.; Li, Y. *J. Am. Chem. Soc.* **2010**, *132*, 3708.

JP909287F